Received: 15 February 2021 | Revised: 23 March 2021 | Accepted: 5 April 2021

DOI: 10.1002/jhet.4271

ARTICLE

JOURNAL OF HETEROCYCLIC CHEMISTRY WILEY

Visible light induced nano copper catalyzed one pot synthesis of novel quinoline bejeweled thiobarbiturates as potential hypoglycemic agents

Gangadhara Angajala[1] | **Valmiki Aruna**[1] | **Radhakrishnan Subashini**[2]

[1]Department of Chemistry, Kalasalingam Academy of Research and Education, Krishnankoil, Tamilnadu, India

[2]Department of Chemistry, Arignar Anna Government Arts College for women, Walajapet, Vellore, Tamilnadu, India

Correspondence
Gangadhara Angajala, Department of Chemistry, Kalasalingam Academy of Research and Education, Anand nagar, Krishnankoil-626126, Tamilnadu, India.
Email: gangadharaangajala@gmail.com

Funding information
VIT University; Kalasalingam Academy of Research and Education

Abstract

An efficient visible light induced one pot three component approach for the synthesis of new quinoline bejeweled thiobarbiturates via Knoevenagel condensation and *N*-alkylation using copper nanoparticles (CuNPs) have been reported. These copper nanoparticles due to their diverse properties, smaller size (50–100 nm), and high surface area to volume ratio exhibit promising features for the reaction response such as the shorter reaction time, simple work-up procedure, clean reaction profiles, and excellent product yields through reusability of the catalyst upto five cycles. The recovered catalyst was successfully characterized by EDAX and AFM analysis. In silico molecular docking studies were carried out to find out the effective binding affinity of the synthesized quinoline derivatives toward PPARγ protein. The results obtained showed that compounds **4d**, **4e**, and **4f** possess good binding interaction toward PPARγ with binding energy of −7.4, −7.2 and, −7.6 k.cal/mol which was greater than standard rosiglitazone (−6.4 k.cal/mol) and comparable to that of standard pioglitazone (−7.9 k.cal/mol). In vitro α-amylase and α-glucosidase assays were performed for hypoglycemic activity evaluation. The compounds **4e** and **4f** at a concentration of 100 μg/ml showed 82.13% and 83.26% inhibition toward α-glucosidase, 78.30% and 84.18% inhibition toward α-amylase which was higher than standard pioglitazone and on par to that of rosiglitazone and acarbose.

KEYWORDS

hypoglycemic, molecular docking, nano copper, PPARγ, quinoline, thiobarbituric acid, visible light

1 | INTRODUCTION

Quinolines scaffold has become an important motif among various heterocycles with interesting biological properties. In recent years quinoline and its congeners have attracted synthetic medicinal chemists because of their prevalence in a variety of natural and pharmacologically active synthetic compounds [1–4]. Quinolines have become important compounds because of their variety of applications in medicinal, synthetic organic chemistry as well as in the field of industrial chemistry [5–9]. Quinoline nucleus is endowed with a variety of therapeutic activities and new quinolone derivatives are known to be biologically active compounds possessing several pharmacological activities being used as antimalarial [10–12], antiviral [13,14], anti-inflammatory [15,16], antiprotozoal

[17–19], antibacterial [20–22], antineoplastic [23,24], antioxidant [25,26], antifungal [27,28], analgesic [29,30], cardiovascular [31], and hypoglycemic agent [32,33]. Considering the noteworthy applications in the fields of bioorganic, medicinal, industrial, and synthetic organic chemistry there has been remarkable interest in developing established protocols for their construction and effective methods for the synthesis of quinolines [34–38].

Similarly, barbituric acid derivatives have shown tremendous attention in the field of medicine due to their potential pharmacological activity over the past few decades [39]. Barbiturates one of the most interesting derivatives of pyrimidines comprise an important valuable group of synthetic compounds particularly effective on the central nervous system [40]. Thiobarbiturates are considered as active agonists toward PPARγ protein [41,42]. In the field of molecular biology, peroxisome proliferator activated receptors (PPARs) constitutes an important group known as nuclear receptor proteins which involve in regulating the expression of genes [43,44] cellular differentiation, metabolism of carbohydrates, lipid, protein as well as tumor genesis in case of higher organisms (Figure 1) [45–47]. Thus PPARγ is considered to play a dual role as possible molecular target in the treatment of cancer and diabetes.

Literature search reveals that only little amount of work has been published on the condensation reaction of quinoline and thiobarbituric acid derivatives. Keeping in view of the affinity of thiobarbituric derivatives with PPARγ receptor and various biological activities associated with quinoline molecule we consider the thiobarbituric acid and quinoline moieties as candidate scaffolds for the synthesis of new therapeutic hypoglycemic agents for type-II diabetes (Figure 2).

Discovery and application of new reagents and reactions has always been the most fascinating aspect of synthetic organic chemistry. Development of novel synthetic methodologies offers a great challenge for organic chemists. In recent years, nano catalysis has received significant attention in organic chemistry because of their greater selectivity, enhanced reaction rates, simple work-up and recoverability of catalysts [48–51]. The application of nano sized catalysts in heterogeneous organic synthesis has numerous advantages such as safe handling, high atom efficiency, shorter reaction time, easy recovery, and recyclability of the catalysts [52–54]. Also, multicomponent reactions (MCRs) have emerged as a successful tool that helps blending the economic aspects with the environmental ones [55,56]. Both metal nanoparticles and MCRs have manifested themselves as synthetic strategies for the rapid introduction, expansion of molecular diversity, and even broaden the scope of combinatorial chemistry [57–59].

In synthetic organic chemistry, Knoevenagel condensation is considered as one of the common significant and extensively followed methods for the construction of carbon–carbon double bond [60–62]. As a result of their significance, enormous number of methods have been reported for Knoevenagel condensation employing various bases [63,64] Lewis acids [65–67] modified inorganic

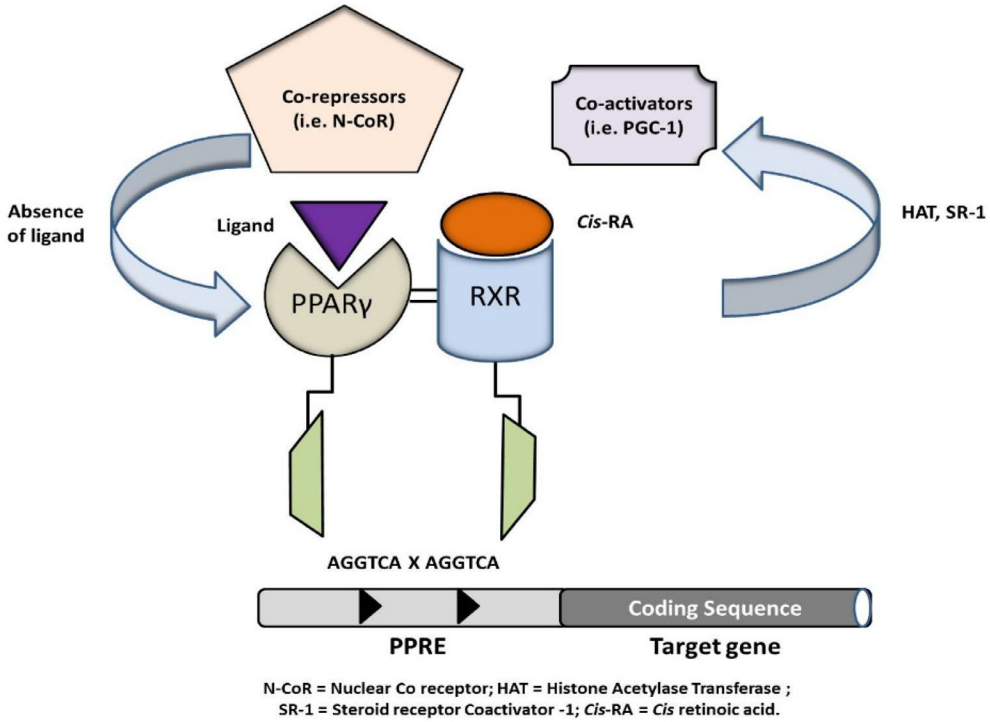

FIGURE 1 Binding of ligand to the PPARγ and the observed cascade

solids [68–71] amino acids [72] ionic liquids [73] palladium-nickel nanoparticles [74] and dendritic copper powder as catalysts [75]. In addition to this, a new light mediated Knoevenagel condensation has also been reported in literature by using aqueous ethanol [76]. It is important to notice that all these procedures have some disadvantages, such as the utilization of costly catalyst, disposal of toxic solvents and catalyst, high temperature conditions, more reaction time frequently generates a problem. The present work was mainly focused to explore the feasibility of copper nano catalyst as an eco-friendly, inexpensive- and effective catalyst for one pot three component synthesis of new quinoline scaffold derived thiobarbiturates through Knoevenagel condensation and N-alkyaltion.

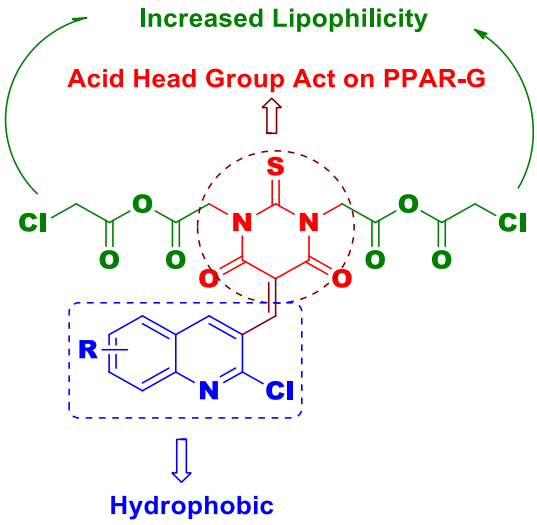

FIGURE 2 Quinoline substituted thiobarbituric acid derivatives as potential hypoglycemic agents

2 | RESULTS AND DISCUSSION

The outline for the preparation of quinoline substituted thiobarbiturates **4a-i** is illustrated in Figure 3. The compounds were prepared by the Knoevenagel condensation of various 2-chloroquinoline-3-carbaldehyde, **1a-i** thiobarbituric acid, **2** and their N-alkylation with chloroacetic anhydride, **3** in the presence of CuNPs as a catalyst under irradiation with tungsten lamp by using ethanol as a solvent medium. As discussed earlier the efficiency of heterogenous catalysis can be improved by employing metal nanoparticles which efficiently catalyzes various organic transformations.

FT-IR spectrum of CuNPs shows the presence of broad band appeared at 3446.79 cm^{-1} which shows the presence of —OH functional groups. Besides high surface to volume ratio, the surface functional hydroxyl groups of the copper nano catalyst (50–100 nm) derived from aqueous leaf extract of *Aegle marmelos* Correa expected to play a dominant role in the synthesis of quinoline substituted thiobarbiturates (see Figure 4).

Hence keeping these facts in mind, our work was initially started with the optimization of the reaction conditions with various concentrations of CuNPs as a catalytic medium by taking (Z)-2-(3-(2-[2-chloroacetoxy]-2-oxoethyl)-5-([2-chloro quinoline-3-yl]methylene)-4,6-dioxo-2-thioxotetrahydro pyrimidin-1(2*H*)-yl)acetic 2-chloroacetic anhydride, **4a** as a model example which was synthesized by the Knoevenagel condensation of 2-chloroquinoline-3-carbaldehyde, **1a** with thiobarbituric acid, **2** followed by N-alkylation in presence of chloroacetic anhydride, **3** as alkylating agent. The compound **4a** was confirmed from ^{1}H NMR spectra which displays 5 protons in the aromatic region and the peak centered at δ 7.27 ppm signifies olefenic proton of the condensed product. The four methylene protons of the *N*-alkylated product

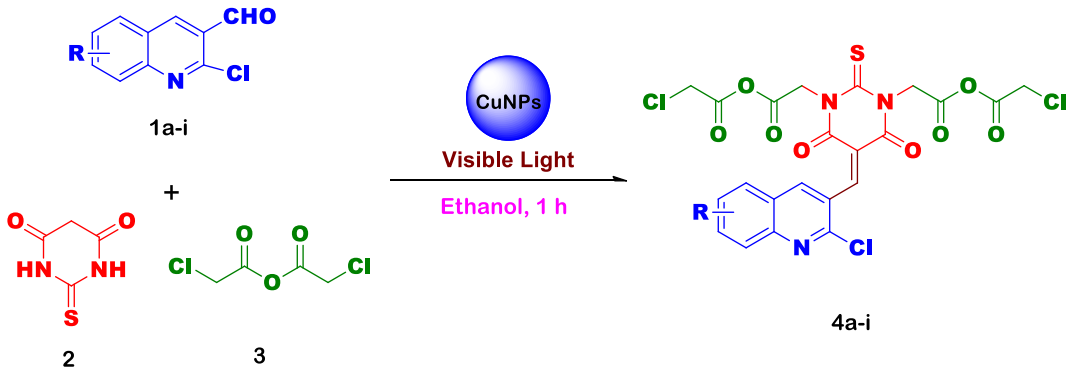

FIGURE 3 Synthesis of new quinoline substituted thiobaribituates **4a-i**

appear assinglets at δ 3.46 and δ 3.22 ppm respectively. The ^{13}C NMR spectrum of compound **4a** revealed 22 carbons in which the —C═S of thiobarbituric acid displayed peak at 197.45 ppm and the peaks at 172.54, 167.26, 163.71 ppm related to carbonyl groups. In addition, the compound **4a** was affirmed by HRMS, which showed the molecular ion peak at m/z 584.9530 (see, Figure S1–S3 in supporting information).

In order to evaluate scope and limitation of the reaction the catalytic effect of CuNPs under visible light in the synthesis of compound **4a** were explored. The loading of the CuNPs was varied and optimized as 10 mol% to afford the corresponding product **4a** in 92% yield deprived of any side products (see Table 1). However, there is no increment in the product yield on further increase in the concentration of the catalyst. The reaction did not proceed even at a longer reaction time in the absence of copper nano catalyst. After screening the catalytic effect the reaction was further elucidated for the role of solvents. During the progress of the reaction, the most significant property of solvent molecules is its ability to respond to the changes connected with charges and their equivalent distribution. From the results it has been found that CuNPs catalyzed Knoevenagel condensation followed by N-alkylation in high yields in the presence of ethanol as a solvent medium (see Table 2).

Considering the optimized reaction conditions in hand, the scope of the protocol was further monitored for the reaction of variety of bases. The effect of bases in the synthesis product **4a** was monitored and compared with that of CuNPs (Table 3). The results obtained gives a clear idea that when compared to bases, CuNPs gave better yields with shorter reaction time (60 min) toward the formation of **4a**. The three component approach through Knoevenagel condensation reaction followed by *N*-alkylation was efficiently carried out with high selectivity by CuNPs as a catalyst under reflux condition with ethanol as a solvent has been chosen for further study. After the completion of the reaction, the catalyst was filtered off from the reaction mixture and thoroughly washed with hot ethanol and water, dried, and activated at 250°C for 3 h.

Finally, the possibility of recycling CuNPs was examined on the reaction of 2-chloroquinoline-3-carbaldehyde, **1a** with thiobarbituric acid, **2** in presence of chloroacetic anhydride, **3** as alkylating agent to afford Knoevenagel condensed, N-alkylated product. The copper nanocatalyst was recovered successfully with recovery percentage of 99%, 99%, 98%, 95%, and 92% respectively for five cycles. Similarly, the recovered nano catalyst reused as such for subsequent experiments up to five cycles under similar reaction conditions. It was observed that the isolated yields of the product were

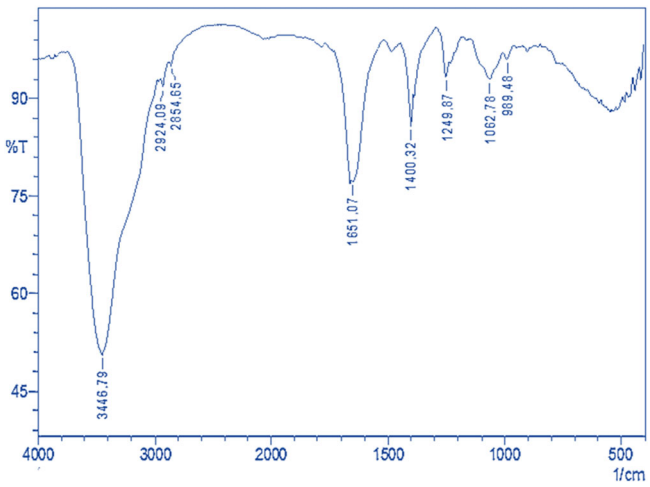

FIGURE 4 FT-IR spectrum of biosynthesized CuNPs (50–100 nm)

TABLE 1 Effect of catalyst concentration in the synthesis of **4a**[a]

S. no	Catalyst (Mol %)	Mode of reaction	Time (min)	Yield (%)[b]
1	2.5	Visible light	320	38
2	5.0	Visible light	250	54
3	7.5	Visible light	125	70
4	10.0	Visible light	60	92
5	12.5	Visible light	60	92
6	15.0	Visible light	60	92
7	15.0	Room temp stirring	180	85
8	15.0	Reflux	220	78
9	No catalyst	Visible light	360	15

[a]Reaction conditions: 2-chloroquinoline-3-carbaldehyde **1a** (1 mmol), thiobarbituric acid, **2** (1 mmol), Chloroacetic anhydride, **3** (2 mmol), CuNPs (50–100 nm), Ethanol.
[b]Isolated yield.

TABLE 2 Influence of solvent in the synthesis of **4a**[a]

S. no	Solvent	Yield (%)[b]
1	Acetonitrile	73
2	Tetrahydrofuran	76
3	Ethanol	92
4	Dichloromethane	70
5	DCM	75
6	Acetone	34
7	Toluene	72
8	DMSO	83
9	H_2O	10
10	Solventless	17

[a]Reaction conditions: 2-chloroquinoline-3-carbaldehyde **1a** (1 mmol), thiobarbituric acid, **2** (1 mmol), Chloroacetic anhydride, **3** (2 mmol), CuNPs (50–100 nm), Visible light (200 Watt).
[b]Isolated yield.

TABLE 3 Effect of base in the synthesis of **4a**[a]

S. no	Base	Yield (%)[b]
1	Piperidine	74
2	Pyridine	78
3	KOH	70
4	Et_3N	71
5	K_2CO_3	58
6	DIPEA	75
7	CuNPs	92

[a]Reaction conditions: 2-chloroquinoline-3-carbaldehyde **1a** (1 mmol), thiobarbituric acid, **2** (1 mmol), Chloroacetic anhydride, **3** (2 mmol), Ethanol.
[b]Isolated yield.

similar and remained with no noticeable loss until the fifth recycling, 92%, 92%, 92%, 90%, and 88% (see Figure 5). In addition, the morphology of the CuNPs remains unaffected thus showing recyclability and reusability of the copper nano catalyst in the synthesis of products **4a**-**4i** without any considerable loss in the catalytic activity (Figure 6).

Energy dispersive X-ray (EDX) analysis was used to probe the composition of the copper nanoparticles. The presence of copper nano catalyst was affirmed from the energy bands positioned at 8 and 8.8 keV [K lines] and 0.9 keV [L lines] respectively. The concentration of oxygen and carbon atoms in the EDX analysis of copper nano catalyst is very low before the starting of the reaction. However, increased concentration of carbon and oxygen atoms detected in EDX analysis of the recovered catalyst was primarily due to the interaction with solvent during the workup process and partial oxidation of the catalyst during handling (see Figure 7A,B). The recovered copper nano catalyst was further characterized by using atomic force microscopy which clearly shows the irregular copper nanoparticles and the presence of corresponding copper nano island (Figure 8). The results obtained from molecular docking simulations of compounds **4a**-**i** with PPARγ protein displayed the effective binding affinities of compound **4d**, **4e**, and **4f** with binding energies of −7.4, −7.2, and −7.6 k.cal/mol which was better than standard rosiglitazone (−6.4 k.cal/mol) and comparable to that of standard pioglitazone (−7.9). The compounds **4b**, **4g**, and **4i** possess moderate binding affinity with PPARγ receptor having binding energies −6.4, −6.3, and −6.7 k.cal/mol (see Table 4, Figure 9A–F, and 10A–E).

The results obtained from enzyme inhibition assays toward hypoglycemic activity revealed that out of the

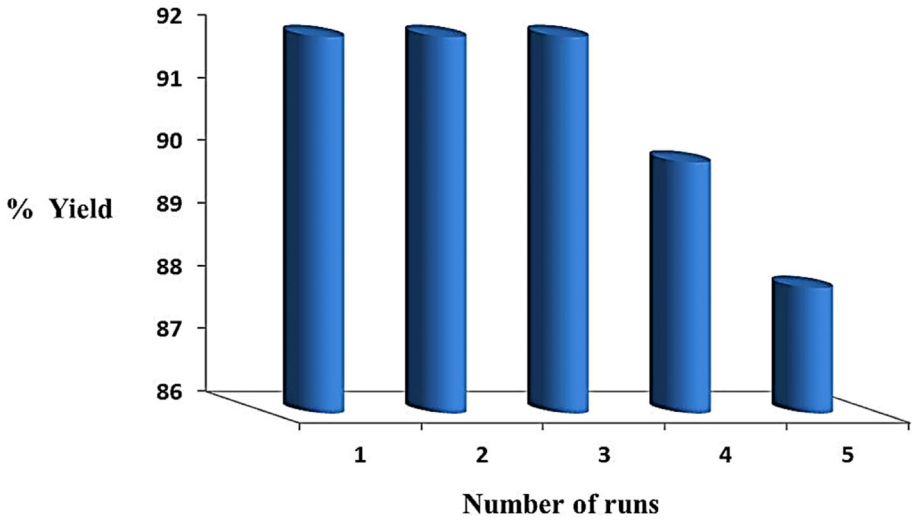

FIGURE 5 Reusability of the CuNPs (50–100 nm)

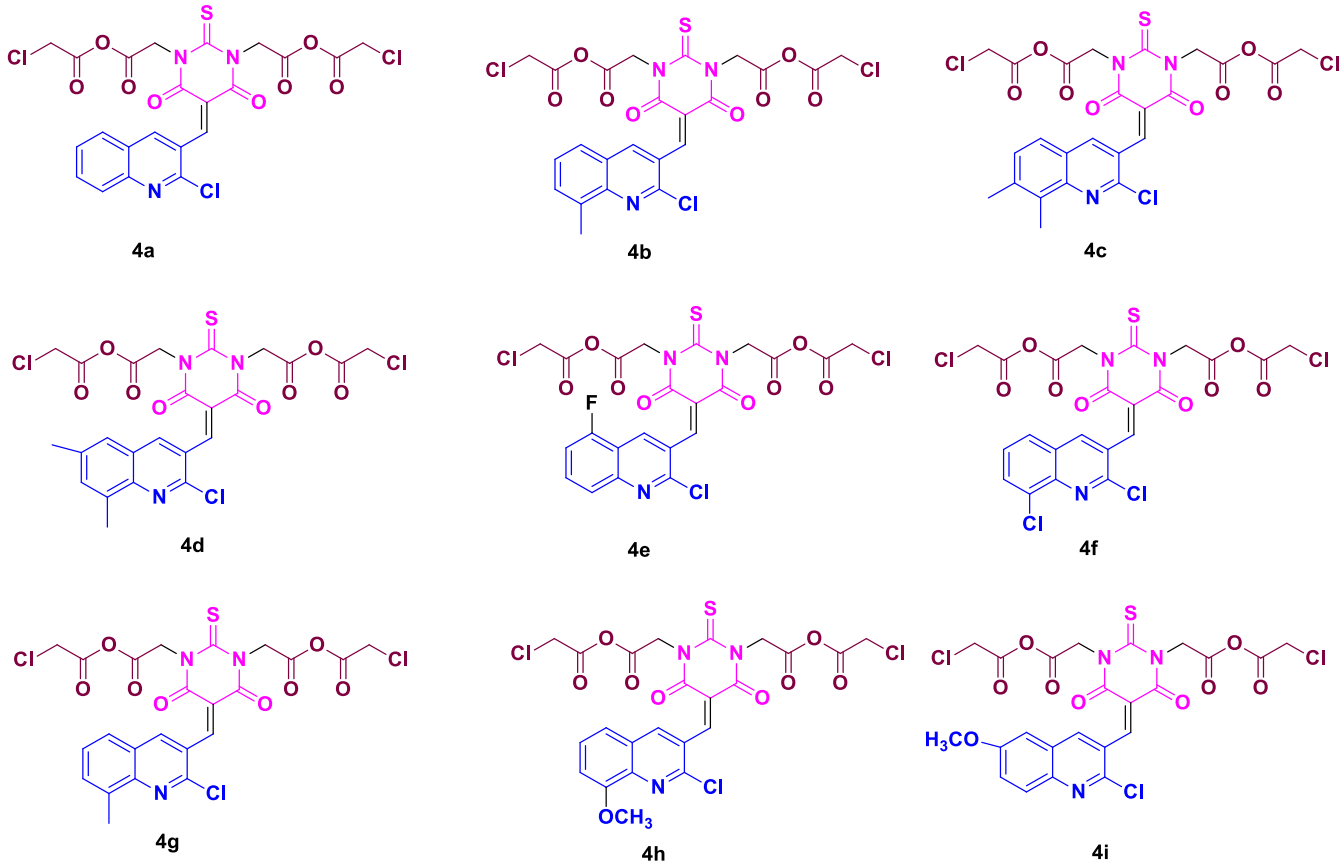

FIGURE 6 Quinoline substituted thiobarbituric acid derivatives (**4a-i**)

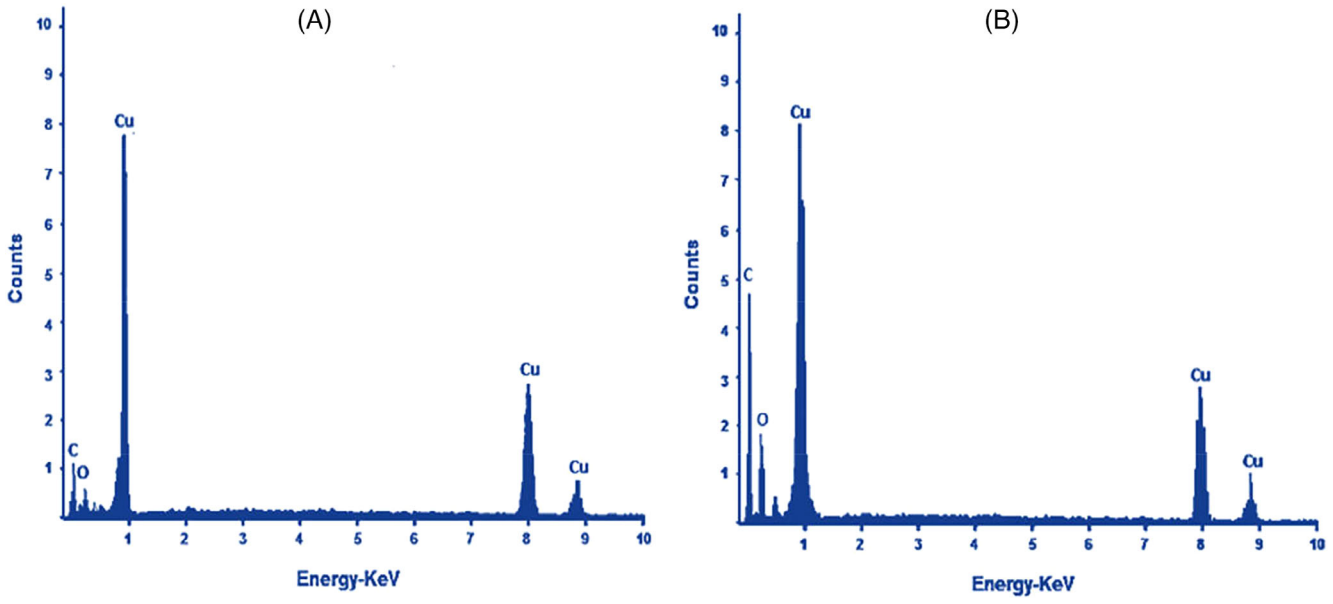

FIGURE 7 (A) EDX analysis of copper nano catalyst (before reaction) (B) EDX analysis of copper nano catalyst (after reaction)

synthesized quinoline derivatives **4a-i** compounds **4e** and **4f** showed 82.13 ± 0.06 and 85.26 ± 0.02 percent inhibition toward α-glucosidase, 78.30 ± 0.82 and 84.19 ± 0.05 percent inhibition toward α-amylase which was greater than standard pioglitazone (74.06 ± 0.07, 73.62 ± 0.05) and comparable to Rosiglitazone (89.70 ± 0.66, 88.14 ± 0.12), Acarbose (91.26 ± 0.41, 90.05 ± 0.62) (see Table 5, 6, Figure 11, and 12). The hypoglycemic efficacy of compounds **4e** and **4f** could be attributed because of the presence of halogens which increases the lipophilicity

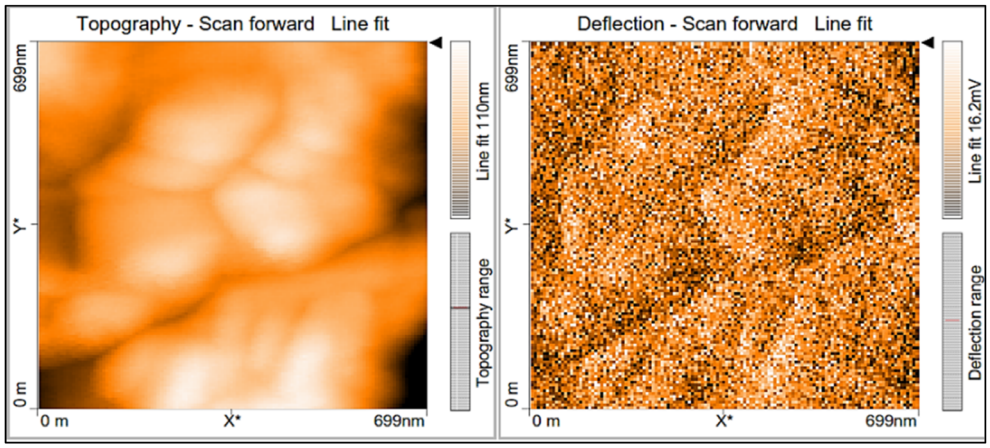

FIGURE 8 The topographical images of the recovered copper nano catalyst

TABLE 4 Binding affinity energies (kcal/Mol) of compounds **4a-i** with PPARγ

S. no	Ligand	Autodock score	Lipophilicity	Hydrophobicity
1	4a	−4.8	−1.6	−0.6
2	4b	−6.4	−2.2	−0.8
3	4c	−5.5	−2.0	−1.2
5	4d	−7.4	−3.0	−1.0
6	4e	−7.2	−2.8	−0.5
7	4f	−7.6	−3.3	−0.3
8	4g	−6.3	−2.5	−1.0
9	4h	−6.1	−1.2	−0.9
10	4i	−6.7	−1.4	−0.7
12	Std[a]	−6.4	−3.9	−0.5
13	Std[b]	−7.9	−4.5	−0.2

[a]Rosiglitazone.
[b]Pioglitazone.

of the compound. Halogens generally increase the ability of molecules to interact with lipophilic unipolar media by allowing stronger London forces. The lower efficacy of the fluoro substituted quinoline derivative **4e** when compared to chloro substituted derivative **4f** was primarily attributed to the high electronegativity and low polarizability of fluorine.

3 | EXPERIMENTAL

3.1 | Materials and method

Reagents and solvents were sourced commercially from Merck and Aldrich and used without further purification. The ^{1}H NMR and ^{13}C NMR for compounds **4a-i** were obtained using a Bruker Avance-400 MHz spectrometer in $CDCl_3$ solvent with Trimethylsilane (TMS) as the internal standard and JEOL GC Mate-II was used to record HRMS spectra. The UV–Visible spectra were recorded using Schimadzu UV spectrophotometer, model UV-1800.

3.1.1 | Biosynthesis of copper nano catalyst

The biosynthesis of copper nano catalyst (50–100 nm) from *Aegle marmelos* Correa aqueous leaf extract was reported in our previous work [77] [Figure 13].

3.1.2 | General procedure for the synthesis of (Z)-2-(3-(2-[2-chloroacetoxy]-2-oxoethyl)-5-([2-chloroquinolin-3-yl] methylene)-4,6-dioxo-2thioxo-tetrahydropyrimidin-1(2*H*)-yl)acetic2 chloro acetic anhydride, 4a

In a round bottom flask a mixture of 2-chloroquinoline-3-carbaldehyde **1a** (1 mmol) which was synthesized according to the reported method by Otto-Meth-Cohn et al. [78] (Refer supporting data S1), thiobarbituric acid, **2** (1 mmol) and chloroacetic anhydride, **3** (2 mmol) was taken. To this mixture catalytic amount of CuNPs

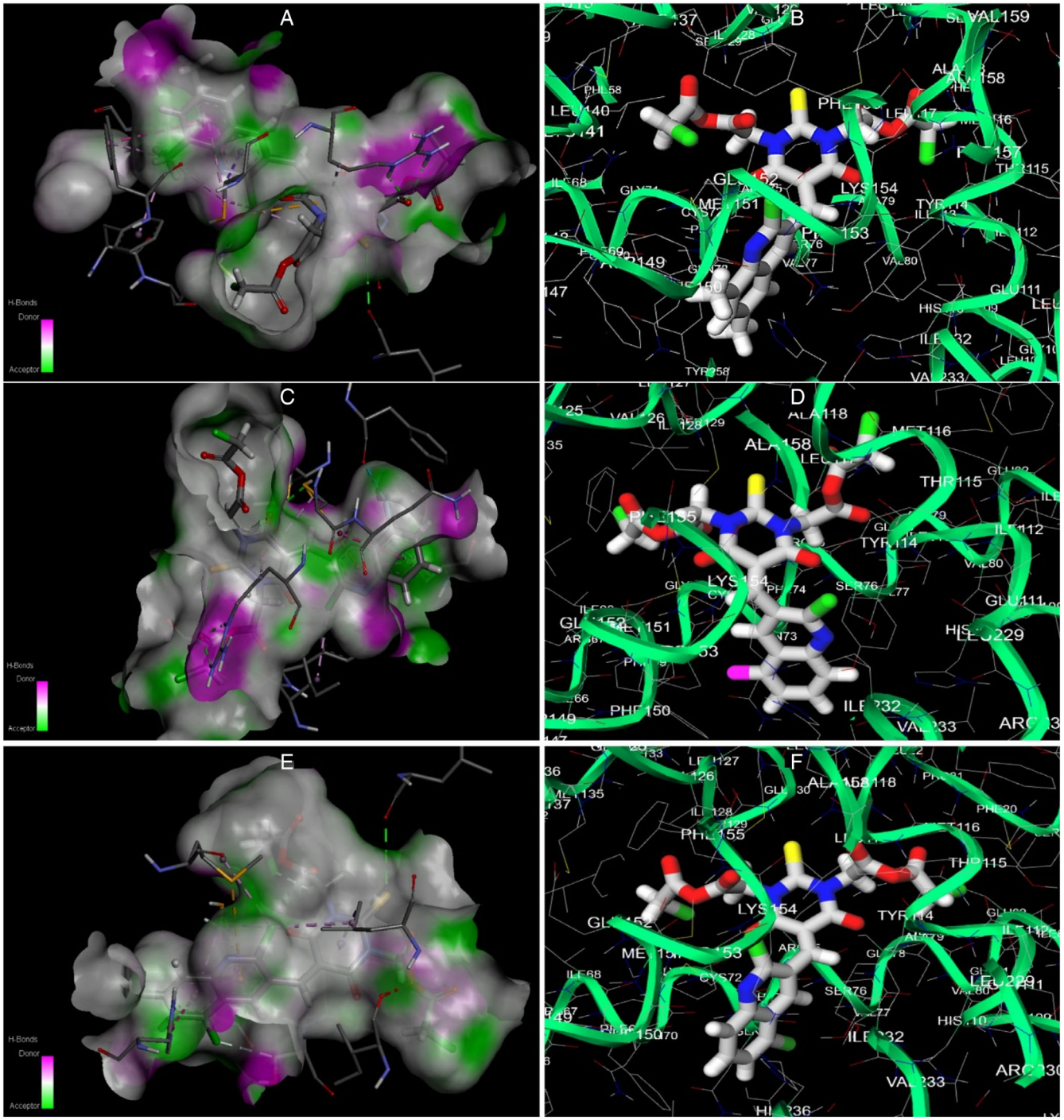

FIGURE 9 Molecular docking simulations of quinoline derivatives **4a**-**i** as hypoglycemic agents (A, B) the binding interaction of **4d** with PPARγ receptor (C, D) the binding interaction of **4e** with PPARγ receptor (E, F) the binding interaction of **4f** with PPARγ receptor

(10 mol %) was added and the whole mixture was irradiated with tungsten lamp (200 Watt) in the presence of ethanol (6 ml) as a solvent. Upon reaction completion (TLC, Petroleum ether: Ethyl acetate, 3:1) the catalyst was filtered off from the reaction medium. The solution was decanted into the beaker and the precipitate was filtered, dried, and further purified using column chromatography to afford compound **4a**.

3.2 | Biological evaluation

3.2.1 | In silico molecular docking studies

The binding affinity of quinoline substituted thiobarbiturates **4a**-**i** with peptide PPARγ were calculated by using Autodock.v.4.2 [79]. The protein structure

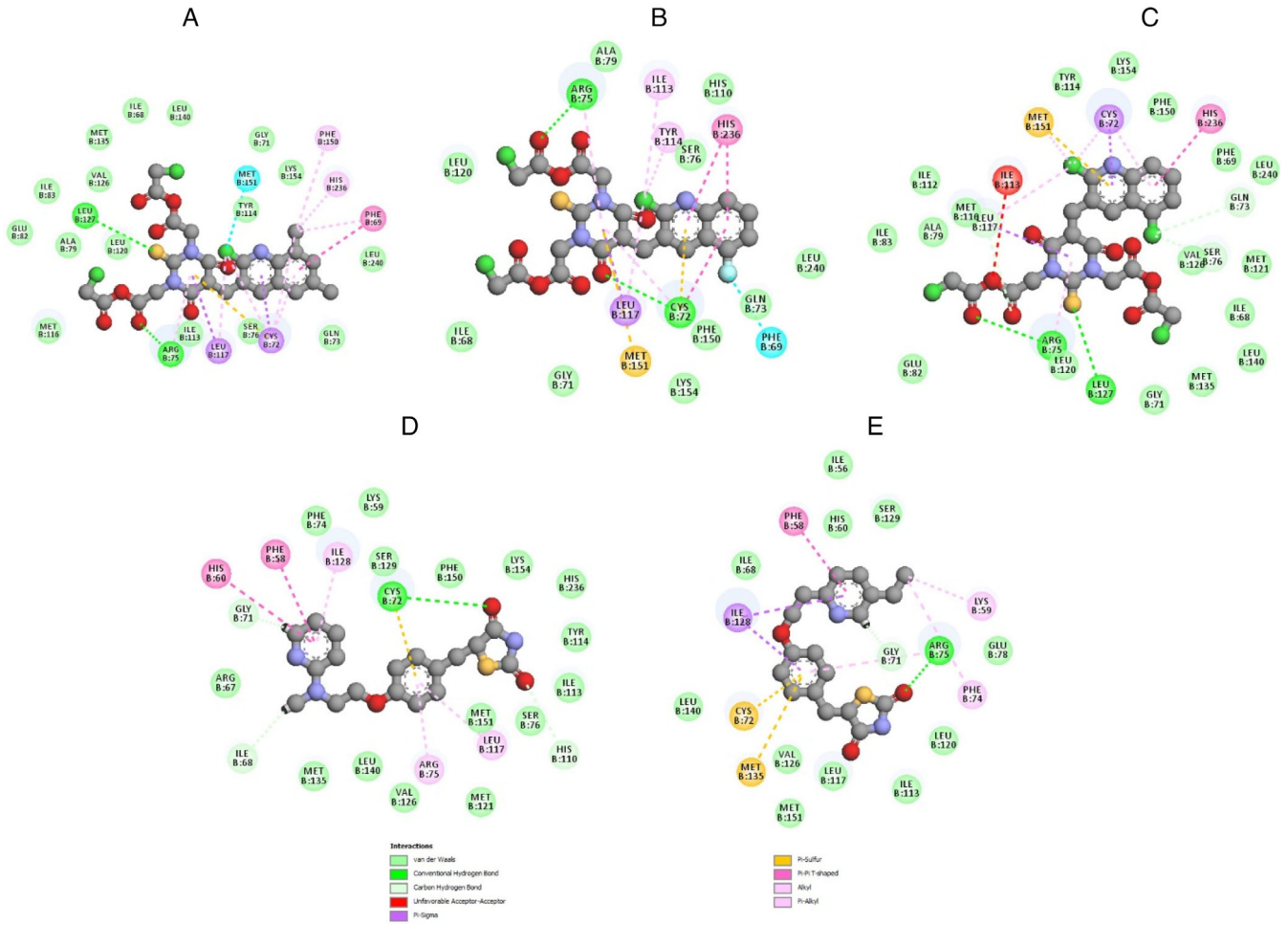

FIGURE 10 Binding interactions of quinoline derivatives and standards with various amino acids of the PPARγ receptor in 2D structural view (A) binding interactions of compound **4d** (B) binding interactions of compound **4e** (C) binding interactions of compound **4f** (D) binding interactions of standard rosiglitazone (E) binding interactions of standard pioglitazone

PPARγ was retrieved from RCSB PDB (PDBID - 2XKW). From Autodock vina under protein preparation, Gasteiger Partial charges and further Hydrogens were added. The docking of ligand to PPARγ was focused on the specific binding site. The number rotatable bonds of the ligands were calculated. The atomic affinity potential and energy of interaction of each atom in the ligand was evaluated. The grid maps were defined to the binding site of PPARγ by setting the configurations along X/Y/Z coordinates. The Binding energies between receptor and the ligands are attained in terms of Kcal/mol. The various drug receptor interactions were analyzed using Accelrys Discovery Studio Visualizer software.

3.2.2 | In vitro hypoglycemic studies

In vitro hypoglycemic efficacy of the synthesized quinoline substituted thiobarbiturates **4a-i** were carried out as per the previous reported methods by using α-amylase [80] and α-glucosidase assays [81] (Refer supporting information S1).

3.3 | Spectral data of the synthesized compounds, (4a-i)

3.3.1 | (Z)-2-(5-([2-chloroquinolin-3-yl] methylene)-3-(2-[2-chloroacetoxy]-2-oxoethyl)-4,6-dioxo-2-thioxotetrahydropyrimidin-1(2*H*)-yl) acetic 2-chloroacetic anhydride, (4a)

Creamish white solid, 92.0% yield, mp 281–283°C. IR (KBr pellets, cm^{-1}) υ: 754.18, 1080.22, 1105.981278.02, 1354.07, 1710.55, 3074.16. ^{1}H NMR ($CDCl_3$, ppm, 400 MHz) δ: 3.22 (4H, s, 2 x CH_2), 3.46 (4H, s, 2 x CH_2), 7.17–7.19 (1H, d, J = 7.2 Hz, CH_2),

TABLE 5 α-Glucosidase inhibitory efficacy of compounds (**4a**-**i**)

S. no	Compound	Concentration (μg/ml)		
		50	100	250
1.	4a	20.13 ± 0.16	39.31 ± 0.78	63.12 ± 0.04
2.	4b	28.15 ± 0.49	45.01 ± 0.08	68.95 ± 1.44
3.	4c	22.18 ± 0.11	41.02 ± 1.32	66.28 ± 0.09
4.	4d	17.05 ± 1.01	25.01 ± 0.08	40.31 ± 0.64
5.	4e	31.02 ± 0.15	54.22 ± 1.05	82.13 ± 0.06
6.	4f	35.04 ± 0.18	52.07 ± 1.71	85.26 ± 0.02
7.	4g	19.02 ± 0.42	27.62 ± 0.55	44.25 ± 0.19
8.	4h	21.47 ± 0.78	30.18 ± 0.62	49.84 ± 0.11
9	4i	23.96 ± 0.15	38.33 ± 0.20	60.59 ± 0.24
10.	Std1[a]	29.06 ± 0.72	47.21 ± 0.65	74.06 ± 0.07
11.	Std2[b]	37.01 ± 0.05	56.24 ± 0.76	89.70 ± 0.66
12	Std3[c]	39.21 ± 0.12	58.72 ± 1.02	91.26 ± 0.41

[a]Pioglitazone.
[b]Rosiglitazone.
[c]Acarbose.

TABLE 6 α-Amylase inhibitory efficacy of compounds (**4a**-**i**)

S. no	Compound	Concentration (μg/ml)		
		50	100	250
1.	4a	17.98 ± 0.13	34.05 ± 0.28	52.12 ± 0.11
2.	4b	18.17 ± 0.16	37.24 ± 1.33	56.14 ± 0.19
3.	4c	21.43 ± 1.66	40.30 ± 1.27	60.19 ± 0.34
4.	4d	24.71 ± 1.50	43.20 ± 0.38	65.25 ± 1.47
5.	4e	35.29 ± 0.17	54.21 ± 1.44	78.30 ± 0.82
6.	4f	39.70 ± 0.66	57.71 ± 0.41	84.19 ± 0.05
7.	4g	20.18 ± 0.72	39.26 ± 0.30	57.33 ± 0.63
8.	4h	19.40 ± 0.32	38.67 ± 0.54	56.87 ± 0.82
9	4i	22.16 ± 0.15	41.62 ± 0.20	61.36 ± 1.04
10.	Std1[a]	28.11 ± 0.54	46.44 ± 0.15	72.06 ± 0.10
11.	Std2[b]	34.20 ± 0.40	53.81 ± 0.29	85.46 ± 0.63
12	Std3[c]	37.08 ± 0.55	56.04 ± 0.05	88.14 ± 0.18

[a]Pioglitazone.
[b]Rosiglitazone.
[c]Acarbose.

7.27 (1H, s, CH), 7.42–7.45 (2H, t, J = 6.8 Hz, CH), 7.63–7.65 (1H, d, J = 7.6 Hz, CH), 8.09 (1H, s, CH). ^{13}C NMR ($CDCl_3$, ppm, 100 MHz) δ: 32.48, 37.92, 116.35, 122.56, 124.83, 125.31, 126.12, 131.14, 133.48, 134.15, 136.51, 137.67, 141.81, 145.39, 147.20, 151.74, 163.71, 167.26, 172.54, 197.45. HRMS [EI$^+$] Calcd for $C_{22}H_{14}Cl_3N_3O_8S$ m/z 584.9567 [M$^+$], found 584.9530 [M$^+$].

3.3.2 | (Z)-2-(5-([2-chloro-8-methylquinolin-3-yl]methylene)-3-(2-[2-chloroacetoxy]-2-oxoethyl)-4,6-dioxo-2-thioxotetrahydropyrim- idin-1(2*H*)-yl) acetic 2-chloroacetic anhydride, (4b)

Pale yellow solid, 90% yield, mp 241°C. IR (KBr pellets, cm^{-1}) υ: 747.29, 1074.05, 1101.561272.47, 1348.10,

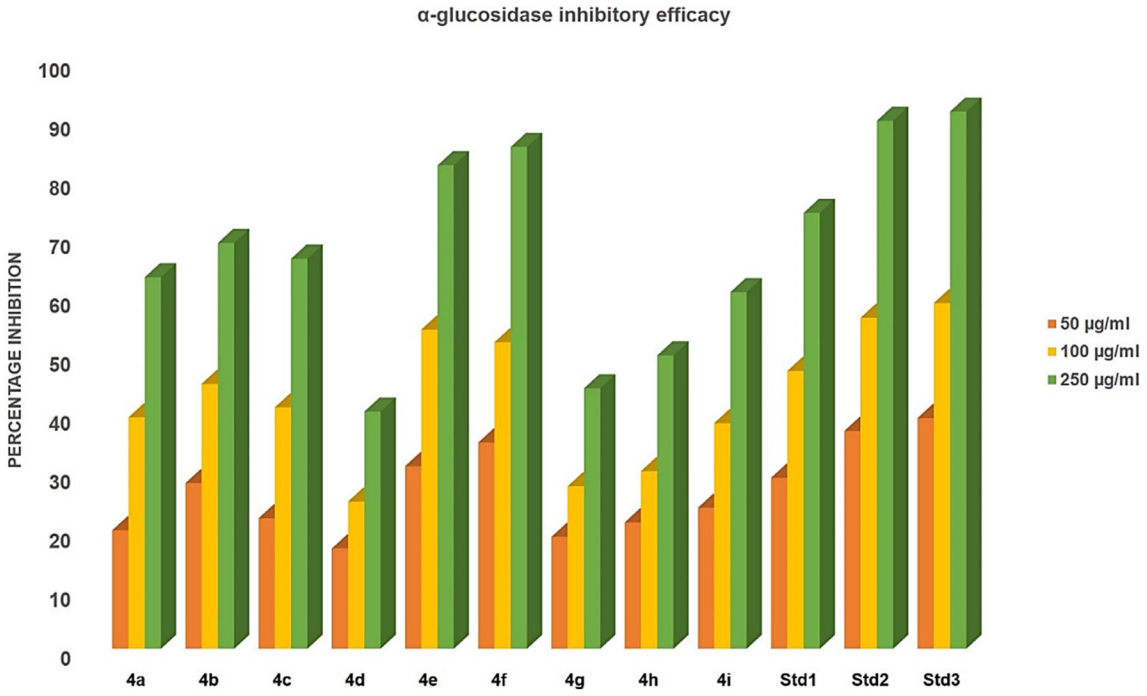

FIGURE 11 α-Glucosidase inhibitory efficacy of quinoline bejeweled thiobarbiturates (**4a**-**i**)

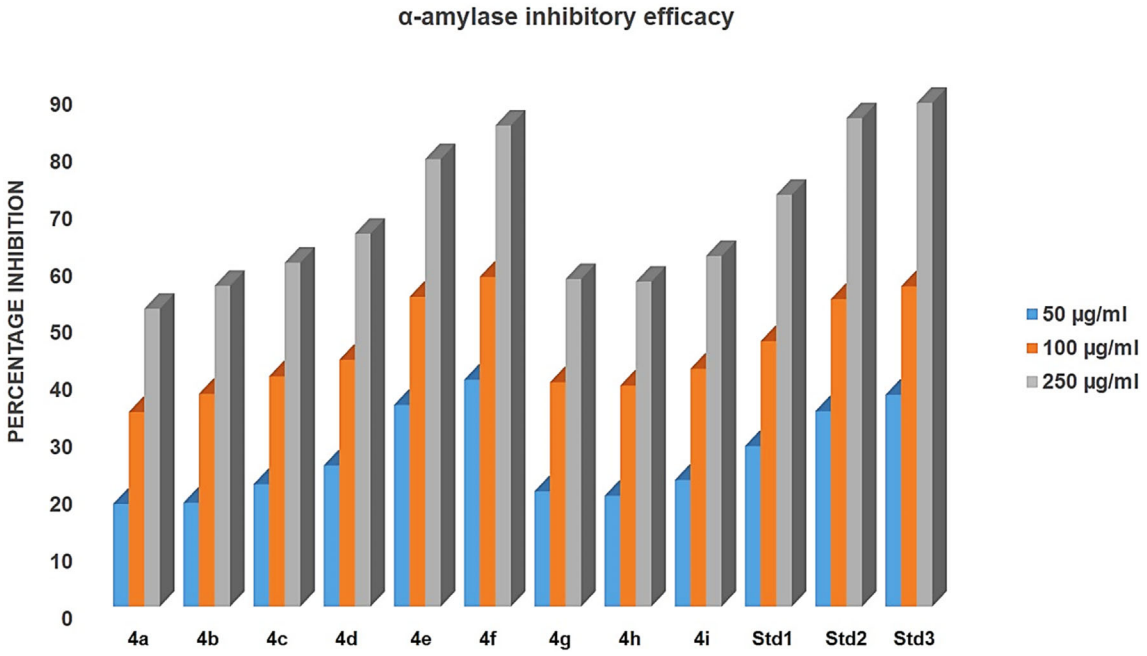

FIGURE 12 α-Amylase inhibitory efficacy of quinoline bejeweled thiobarbiturates (**4a**-**i**)

1705.14, 3077.28. ^{1}H NMR ($CDCl_3$, ppm, 400 MHz) δ: 2.59 (3H, s, CH_3), 3.45 (4H, s, 2 x CH_2), 3.62 (4H, s, 2 x CH_2), 7.28 (1H, s, CH), 7.36–7.42 (1H, d, J = 6.4 Hz, CH), 7.50–7.56 (1H, q, J = 4.4 Hz, CH), 7.68–7.69 (1H, d, J = 4.8 Hz, CH), 7.92–7.93 (1H, d, J = 7.2 Hz, CH). ^{13}C NMR ($CDCl_3$, ppm, 100 MHz) δ: 21.79, 35.63, 41.75, 109.22, 122.89, 124.78, 125.21, 128.05, 129.56, 133.65, 139.65, 143.12, 143.55, 146.93, 151.70, 166.14, 169.25, 175.02, 201.29. HRMS [EI$^+$] Calcd for $C_{23}H_{16}Cl_3N_3O_8S$ m/z 598.9724 [M$^+$], found 598.9730 [M$^+$].

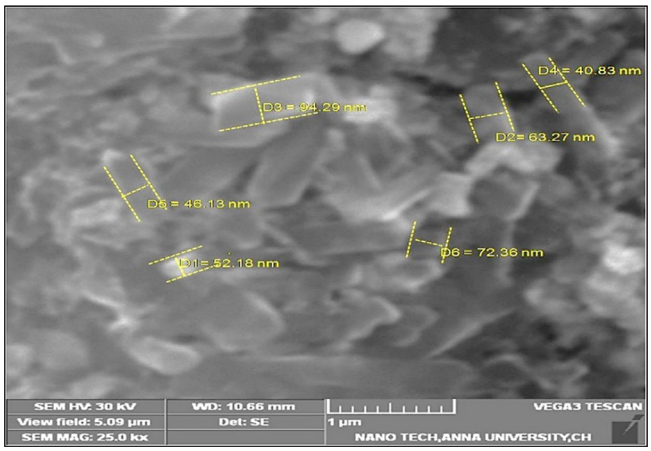

FIGURE 13 SEM image of the CuNPs (50–100 nm)

3.3.3 | (Z)-2-(5-([2-chloro-7,8-dimethylquinolin-3-yl]methylene)-3-(2-[2-chloroacetoxy]-2-oxoethyl)-4,6-dioxo-2-thioxotetrahydro pyrimidin-1(2*H*)-yl) acetic 2-chloroacetic anhydride, (4c)

Pale brown solid, 90.0% yield, mp 274–276°C. IR (KBr pellets, cm^{-1}) υ: 748.25, 1075.44, 1102.071274.82, 1350.20, 1708.71, 3072.06. ^{1}H NMR ($CDCl_3$, ppm, 400 MHz) δ: 2.38 (3H, s, CH_3), 2.54 (3H, s, CH_3), 3.62 (4H, s, 2 x CH_2), 3.91 (4H, s, 2 x CH_2), 7.18–7.21 (1H, d, J = 6.2 Hz, CH), 7.37 (1H, s, CH), 7.48 (1H, s, CH), 8.19 (1H, s, CH). ^{13}C NMR ($CDCl_3$, ppm, 100 MHz) δ: 17.54, 21.34, 38.40, 42.64, 117.22, 121.72, 123.45, 124.83, 125.97, 132.69, 134.06, 135.27, 137.02, 138.15, 14,033, 146.49, 147.83, 152.91, 165.04, 171.22, 176.43, 202.06. HRMS [EI$^+$] Calcd for $C_{24}H_{18}Cl_3N_3O_8S$ m/z 612.9880 [M^+], found 612.9827 [M^+].

3.3.4 | (Z)-2-(5-([2-chloro-6,8-dimethylquinolin-3-yl]methylene)-3-(2-[2-chloroacetoxy]-2-oxoethyl)-4,6-dioxo-2-thioxotetrahydro pyrimidin-1(2*H*)-yl) acetic 2-chloroacetic anhydride, (4d)

Off white solid, 88.0% yield, mp 257–258°C. IR (KBr pellets, cm^{-1}) υ: 745.38, 1072.61, 1101.77, 1275.81, 1348.15, 1710.03, 3062.84. ^{1}H NMR ($CDCl_3$, ppm, 400 MHz) δ: 2.21 (3H, s, CH_3), 2.75 (3H, s, CH_3), 3.38 (4H, s, 2 x CH_2), 3.60 (4H, s, 2 x CH_2), 7.13–7.15 (1H, d, J = 7.6 Hz, CH), 7.30 (1H, s, CH), 7.43 (1H, s, CH), 8.02 (1H, s, CH). ^{13}C NMR ($CDCl_3$, ppm, 100 MHz) δ: 17.92, 22.48, 37.66, 41.48, 116.35, 122.56, 124.83, 125.31, 126.12, 131.14, 133.48, 134.15, 136.51, 137.67, 141.81, 145.39, 147.20, 151.74, 164.65, 170.89, 175.59, 201.44. HRMS [EI$^+$] Calcd for $C_{24}H_{18}Cl_3N_3O_8S$ m/z 612.9880 [M^+], found 612.9835 [M^+].

3.3.5 | (Z)-2-(5-([2-chloro-5-fluoroquinolin-3-yl]methylene)-3-(2-[2-chloroacetoxy]-2-oxoethyl)-4,6-dioxo-2-thioxotetrahydro pyrimidin −1(2*H*)-yl) acetic 2-chloroacetic anhydride, (4e)

White solid, 94.0% yield, mp 272°C. IR (KBr pellets, cm^{-1}) υ: 742.10, 1075.26, 1098.65, 1272.80, 1348.27, 1706.14, 3078.10. ^{1}H NMR ($CDCl_3$, ppm, 400 MHz) δ: 3.61 (4H, s, 2 x CH_2), 3.91 (4H, s, 2 x CH_2), 7.45–7.47 (2H, d, J = 8.0 Hz, CH), 7.60–7.65 (2H, t, J = 6.0 Hz, CH), 7.84–7.86 (1H, d, J = 7.6 Hz, CH). ^{13}C NMR ($CDCl_3$, ppm, 100 MHz) δ: 39.68, 40.78, 122.24, 125.20, 126.94, 126.97, 127.83, 131.64, 134.17, 138.13, 140.46, 144.87, 146.05, 146.93, 151.23, 164.93, 169.10, 174.17, 201.53. HRMS [EI$^+$] Calcd for $C_{22}H_{13}Cl_3FN_3O_8S$ m/z 602.9473 [M^+], found 602.9710 [M^+].

3.3.6 | (Z)-2-(5-([2,5-dichloroquinolin-3-yl]methylene)-3-(2-[2-chloroacetoxy]-2-oxoethyl)-4,6-dioxo-2-thioxotetrahydro pyrimidin-1(2*H*)-yl)acetic 2-chloroacetic anhydride, (4f)

Pale brown, 89.0% yield, mp 265–266°C. IR (KBr pellets, cm^{-1}) υ: 745.11, 1072.05, 1103.261270.18, 1345.24, 1708.16, 3075.22. ^{1}H NMR ($CDCl_3$, ppm, 400 MHz) δ: 3.31 (4H, s, 2 x CH_2), 3.79 (4H, s, 2 x CH_2), 7.35–7.37 (1H, d, J = 8.0 Hz, CH), 7.46–7.48 (1H, s, CH), 7.63–7.64 (2H, d, J = 6.8 Hz, CH), 7.92 (1H, s, CH), 8.05–8.06. ^{13}C NMR ($CDCl_3$, ppm, 100 MHz) δ: 39.27, 45.78, 110.22, 121.36, 125.01, 125.15, 125.29, 130.72, 133.41, 133.81, 140.05, 141.12, 144.52, 146.58, 147.24, 152.23, 167.32, 172.45, 176.28, 202.22. HRMS [EI$^+$] Calcd for $C_{22}H_{13}Cl_4N_3O_8S$ m/z 618.9177 [M^+], found 618.9143 [M^+].

3.3.7 | (Z)-2-(5-([2-chloro-6-methylquinolin-3-yl]methylene)-3-(2-[2-chloroacetoxy]-2-oxoethyl)-4,6-dioxo-2-thioxotetrahydro pyrimidin-1(2*H*)-yl) acetic 2-chloroacetic anhydride, (4g)

Light yellow solid, 92% yield, mp 269°C. IR (KBr pellets, cm^{-1}) υ: 756.18, 1078.04, 1106.10, 1276.22, 1346.02, 1710.11, 3074.19. ^{1}H NMR ($CDCl_3$, ppm, 400 MHz) δ:1.72 (3H, s, CH_3), 3.69 (4H, s, 2 x CH_2), 4.10 (4H, s, 2 x CH_2), 7.18 (1H, s, CH), 7.52 (1H, s, CH), 7.64 (1H, s, CH), 7.72–

7.73 (1H, d, $J = 4.4$ Hz, CH), 8.24 (1H, s, CH). ^{13}C NMR ($CDCl_3$, ppm, 100 MHz) δ: 20.52, 34.70, 42.91, 110.51, 121.47, 123.18, 124.10, 129.42, 130.67, 134.71, 140.11, 143.83, 144.07, 147.22, 152.19, 167.26, 170.48, 176.32, 202.18. HRMS [EI$^+$] Calcd for $C_{23}H_{16}Cl_3N_3O_8S$ m/z 598.9724 [M$^+$], found 598.9745 [M$^+$].

3.3.8 | (Z)-2-(5-([2-chloro-6-methoxyquinolin-3-yl]methylene)-3-(2-[2-chloroacetoxy]-2-oxoethyl)-4,6-dioxo-2-thioxotetrahydro pyrimidin-1(2*H*)-yl)acetic 2-chloroacetic anhydride, (4h)

Pale brown solid, 88.0% yield, mp 258°C. IR (KBr pellets, cm^{-1}) υ: 756.18, 1078.84, 1105.42, 1276.04, 1354.22, 1710.90, 3074.03. ^{1}H NMR ($CDCl_3$, ppm, 400 MHz) δ: δ: 3.61 (3H, s, OCH_3), 4.38 (4H, s, 2 x CH_2), 4.65 (4H, s, 2 x CH_2), 7.44–7.50 (1H, q, $J = 6.4$ Hz, CH), 7.52–7.54 (2H, d, $J = 8.0$ Hz, CH), 7.73 (1H, s, CH), 7.91–7.93 (1H, d, $J = 9.2$ Hz, CH_2). ^{13}C NMR ($CDCl_3$, ppm, 100 MHz) δ: 38.22, 40.78, 55.66, 105.10, 122.92, 124.74, 125.10, 128.00, 129.52, 133.61, 139.59, 143.17, 143.50, 146.97, 158.67, 167.01, 173.62, 178.77, 200.37. HRMS [EI$^+$] Calcd for $C_{22}H_{16}Cl_3N_3O_9S$ m/z 614.9673 [M$^+$], found 614.2343 [M$^+$].

3.3.9 | (Z)-2-(5-([2-chloro-8-methoxyquinolin-3-yl]methylene)-3-(2-[2-chloroacetoxy]-2-oxoethyl)-4,6-dioxo-2-thioxotetrahydro pyrimidin-1(2*H*)-yl)acetic 2-chloroacetic anhydride, (4i)

White solid, 90.0% yield, mp 267–269°C. IR (KBr pellets, cm^{-1}) υ: 752.19, 1074.62, 1108.05, 1274.92, 1352.72, 1712.48, 3082.65. ^{1}H NMR ($CDCl_3$, ppm, 400 MHz) δ: 3.24 (3H, s, OCH_3), 4.18 (4H, s, 2 x CH_2), 4.37 (4H, s, 2 x CH_2), 7.52–7.58 (1H, q, $J = 7.2$ Hz, CH), 7.63–7.65 (2H, d, $J = 6.4$ Hz, CH), 7.82 (1H, s, CH), 7.95–7.97 (1H, d, $J = 8.0$ Hz, CH_2). ^{13}C NMR ($CDCl_3$, ppm, 100 MHz) δ: 37.18, 41.62, 56.72, 104.28, 121.83, 123.90, 124.09, 127.25, 130. 19, 132.48, 140.36, 142.68, 144.72, 147.10, 159.03, 168.15, 174.18, 176.98, 201.62. HRMS [EI$^+$] Calcd for $C_{22}H_{16}Cl_3N_3O_9S$ m/z 614.9673 [M$^+$], found 614.2362. Conclusion.

An ecofriendly protocol has been developed for the synthesis of quinoline substituted thiobarbiturates through Knoevenagel condensation and *N*-alkylation by using copper nano catalyst under visible light. The present work explores a highly efficient and environmental friendly approach for the preparation of quinoline substituted thiobarbituric acid derivatives. The outstanding reusability of the catalyst and operational simplicity and high yields are among the other added advantages that make this protocol an attractive alternative route for the synthesis of target hypoglycemic agents. The synergistic effect of both quinoline and *N*-alkylated thiobarbituric acid further enhances the hypoglycemic efficacy of the final target molecules **4a**-**i**. The increase in lipophilicity of the compounds **4e**, **4f** was mainly responsible for showing good hypoglycemic efficacy.

ACKNOWLEDGMENTS

The authors sincerely thank the management of Kalasalingam Academy of Research and Education and VIT University, Tamil Nadu, India for their constant encouragement and support and providing all the necessary facilities for carrying out this research work. The authors also thank DST-VIT-FIST, SIF-VIT for carrying out NMR analysis.

CONFLICT OF INTEREST

The authors declare no conflict of interest.

DATA AVAILABILITY STATEMENT

Data available in article supplementary material.

ORCID

Gangadhara Angajala https://orcid.org/0000-0001-5065-5329

REFERENCES

[1] R. D. Larsen, E. G. Corley, A. O. King, J. D. Carrol, P. Davis, T. R. Verhoeven, P. J. Reider, M. Labelle, J. Y. Gauthier, Y. B. Xiang, R. J. Zamboni, *J. Org. Chem.* **1996**, *61*, 3398.
[2] Y. L. Chen, K. C. Fang, J. Y. Sheu, S. L. Hsu, C. C. Tzeng, *J. Med. Chem.* **2001**, *44*, 2374.
[3] G. Roma, M. D. Braccio, G. Grossi, F. Mattioli, M. Ghia, G. Roma, M. D. Braccio, G. Grossi, F. Mattioli, M. Ghia, *Eur. J. Med. Chem.* **2000**, *35*, 1021.
[4] P. M. S. Chauhan, S. K. Srivastava, *Curr. Med. Chem.* **2001**, *8*, 1535.
[5] M. I. Anderson, A. P. MacGowan, *J. Antimicrob. Chemoth.* **2003**, *51*, 1.
[6] H. I. Abd-Alla, M. Shaaban, K. A. Shaaban, N. S. Abu-Gabal, N. M. Shalaby, H. Laatsch, *Nat. Pro. Res.* **2009**, *23*, 1035.
[7] K. Goto, K. Yabe, T. Suzuki, T. Jindoa, A. Sanbuissho, *Toxicology* **2010**, *276*, 122.
[8] P. M. Hawkey, *J. Antimicrob. Chemoth.* **2003**, *51*, 29.
[9] M. Malik, G. Hoatam, K. Chavda, R. J. Kerns, K. Drlica, *Antimicrob. Agents Chemother.* **2010**, *54*, 149.
[10] K. Raynes, M. Foley, L. Tilley, L. W. Deady, *Biochem. Pharmacol.* **1996**, *52*, 551.
[11] L. C. S. Pinheiro, L. M. Feitosa, M. O. Gandi, F. F. Silveria, N. Boechat, *Molecules* **2019**, *24*, 4095.
[12] T. Herraiz, H. Guillen, D. Gonzalez-Pena, V. J. Aran, *Sci. Rep.* **2019**, *9*, 15398.

[13] J. Ghosh, V. Swarup, A. Saxena, S. Das, A. Hazra, P. Paira, S. Banerjee, N. B. Mondal, A. Basu, *Int. J. Antimicrob. Agents* **2008**, *32*, 349.

[14] C. D. L. Guardia, D. E. Stephens, H. T. Dang, M. Quijada, O. V. Larionov, R. Lleonart, *Molecules* **2018**, *23*, 672.

[15] Y. Chen, Y. Zhao, C. Lu, C. Tzeng, J. P. Wang, *Bioorg. Med. Chem.* **2006**, *14*, 4373.

[16] S. K. Gupta, A. Mishra, *Antiinflamm. Antiallergy Agents Med. Chem.* **2016**, *15*, 31.

[17] A. Fournet, A. A. Barrios, V. Munoz, R. Hocquemiller, A. Cave, J. Bruneton, *Antimicrob. Agents Chemother.* **1993**, *37*, 859.

[18] P. Hochegar, J. Faist, W. Seebacher, R. Saf, P. Maser, M. Kaiser, R. Weis, *Med. Chem.* **2019**, *15*, 409.

[19] E. Garcia, J. C. Coa, E. Otero, M. Carda, I. D. Velez, S. M. Robledo, W. I. Cardona, *Med. Chem. Res.* **2018**, *27*, 497.

[20] J. P. Sanchez, J. M. Domagala, S. E. Hagen, C. L. Heifetz, M. P. Hutt, J. B. Nichols, A. K. Trehan, *J. Med. Chem.* **1988**, *31*, 983.

[21] D. Insuasty, O. Vidal, A. Bernal, E. Marguez, J. Guzman, B. Insuasty, J. Quiroga, L. Svetaj, S. Zacchino, G. Puerto, R. Abonia, *Antibiotics* **2019**, *8*, 239.

[22] T. D. M. Pharm, Z. M. Ziora, M. A. T. Blaskovich, *Med. Chem. Commun.* **2019**, *10*, 1719.

[23] D. A. Scott, C. L. Balliet, D. J. Cook, A. M. Davies, T. W. Gero, C. A. Omer, S. Poondru, M. E. Theoclitou, B. Tyurin, M. J. Zinda, *Bioorg. Med. Chem. Lett.* **2009**, *19*, 697.

[24] M. R. Selim, M. A. Zahran, A. Belal, M. S. Abusaif, S. A. Shedid, A. B. M. Mehany, G. A. M. Elhagali, Y. A. Ammar, *Anti-Cancer Agents Med. Chem.* **2019**, *19*, 439.

[25] R. Subashini, G. Angajala, K. Aggile, F. Nawaz khan, *Res. Chem. Intermed.* **2014**, *41*, 4899.

[26] K. Douadi, S. Chafaa, T. Douadi, M. Al-Noaimi, *J. Mol. Struct.* **2020**, *1217*, 128305.

[27] A. R. Gholap, K. S. Toti, F. Shirazi, R. Kumari, M. K. Bhat, M. V. Deshpande, K. V. Srinivasan, *Bioorg. Med. Chem.* **2007**, *15*, 6705.

[28] G. Z. Yang, J. K. Zhu, X. D. Yin, Y. F. Yan, Y. L. Wang, X. F. Shang, Y. Q. Liu, Z. M. Zhao, J. W. Peng, H. Liu, *J. Agric. Food Chem.* **2019**, *67*, 11340.

[29] A. H. Abadi, G. H. Hegazy, A. A. E. Zaher, *Bioorg. Med. Chem.* **2005**, *13*, 5759.

[30] A. Manikandan, S. Ravichandran, K. I. Sathiyanarayanan, A. Sivakumar, *Inflammopharmacology* **2017**, *25*, 621.

[31] R. C. Bernotas, R. R. Singhaus, D. H. Kaufman, J. Ullrich, H. Fletcher, E. Quinet, P. Nambi, R. Unwalla, A. Wilhelmsson, A. G. Nilsson, M. Farnegardh, J. Wrobel, *Bioorg. Med. Chem.* **2009**, *17*, 1663.

[32] D. Edmont, R. Rocher, C. Plisson, J. Chenault, *Bioorg. Med. Chem. Lett.* **2000**, *10*, 1831.

[33] H. W. Lee, J. Y. Yang, H. S. Lee, *J. Korean Soc. Appl. Biol. Chem.* **2014**, *57*, 441.

[34] M. Z. Hoemann, G. Kumaravel, R. L. Xie, R. F. Rossi, S. Meyer, A. Sidhu, G. D. Cuny, J. R. Hauske, *Bioorg. Med. Chem. Lett.* **2000**, *10*, 2675.

[35] V. V. Kouznetsov, L. Y. V. Mendez, C. M. M. Gomez, *Curr. Org. Chem.* **2005**, *9*, 141.

[36] F. Xiao, Y. Chen, Y. Liu, J. Wang, *Tetrahedron* **2008**, *64*, 2755.

[37] P. G. Dormer, K. K. Eng, R. N. Farr, G. R. Humphrey, J. C. McWilliams, P. J. Reider, J. W. Sager, R. P. Volante, *J. Org. Chem.* **2003**, *68*, 467.

[38] M. Matsugi, F. Tabusa, J. Minamikawa, *Tetrahedron Lett.* **2000**, *41*, 8523.

[39] H. Zheng, S. Li, L. Ma, L. Cheng, C. Deng, Z. Chen, C. Xie, M. Xiang, W. Jiang, L. Chen, *Eur. J. Pharmacol.* **2011**, *659*, 244.

[40] J. H. Gardener, F. H. Bopp, R. F. Prindle, *J. Am. Chem. Soc.* **1946**, *68*, 585.

[41] A. Barakat, S. M. Soliman, Y. A. M. M. Elshaier, M. A. Abdullah, M. Al-Majid, H. A. Ghabbour, *J. Mol. Struct.* **2017**, *1134*, 99.

[42] V. A. Dixit, P. C. Rathi, S. Bhagat, H. Gohlke, R. K. Petersen, K. Kristiansen, A. K. Chakraborti, P. V. Bharatam, *Eur. J. Med. Chem.* **2016**, *108*, 423.

[43] K. Yu, W. Bayona, C. B. Kallen, H. P. Harding, C. P. Ravera, G. McMahon, M. Brown, M. A. Lazar, *J. Biol. Chem.* **1995**, *270*, 23975.

[44] J. Berger, D. E. Moller, *Annu. Rev. Med.* **2002**, *53*, 409.

[45] J. N. Feige, L. Gelman, L. Michalik, B. Desvergne, W. Wahli, *Prog. Lipid Res.* **2006**, *45*, 120.

[46] C. Janani, B. D. Ranjitha Kumari, *Diabetes Metab. Syndr. Clin. Res. Rev.* **2014**, *9*, 46.

[47] S. Yasmin, V. Jayaprakash, *Eur. J. Med. Chem.* **2017**, *126*, 879.

[48] A. Maleki, R. Firouji-Haji, *Sci. Rep.* **2018**, *8*, 17303.

[49] A. Corma, H. Garcia, *Catal. Today* **1997**, *38*, 257.

[50] S. K. Sikdar, S. G. J. Howell, *J. Clean. Product.* **1998**, *6*, 253.

[51] L. Liu, A. Corma, *Chem. Rev.* **2018**, *118*, 4981.

[52] G. Angajala, R. Subashini, *RSC Adv.* **2015**, *5*, 45599.

[53] G. M. Whitesides, *Nat. Biotechnol.* **2003**, *21*, 1161.

[54] R. Narayanan, M. A. El-Sayed, *J. Am. Chem. Soc.* **2004**, *126*, 7194.

[55] A. R. Kiasat, S. Noorizadeh, M. Ghahremani, S. F. saghanejad, *J. Mol. Struct.* **2013**, *1036*, 216.

[56] A. V. Artemev, N. K. Gusarova, I. Y. Bagryanskaya, E. P. Doronina, S. I. Verkhoturova, V. F. Sidorkin, B. A. Trofimov, *Eur. J. Inorg. Chem.* **2013**, *2013*, 415.

[57] K. D. Bhatte, K. M. Deshmukh, Y. P. Patil, D. N. Sawant, S. I. Fujita, M. Arai, B. M. Bhanage, *Particuology* **2012**, *10*, 140.

[58] I. Ban, J. Sterger, M. Drofenic, G. Ferk, D. Makovec, *J. Magn. Magn. Mater.* **2011**, *323*, 2254.

[59] X. Zhao, L. Wei, S. Cheng, J. Julson, *Catalysts* **2017**, *7*, 83.

[60] E. Knoevenagel, *Eur. J. Inorg. Chem.* **1894**, *2*, 2345.

[61] E. Knoevenagel, *Eur. J. Inorg. Chem.* **1898**, *31*, 2585.

[62] G. Jones, *Org. React.* **1967**, *15*, 204.

[63] L. F. Tietze, U. Beifuss, The Knoevenagel Reaction. in *Comprehensive Organic Synthesis* (Ed: B. M. Trost), Pergamon Press, Oxford, UK **1991**, p. 341.

[64] B. F. Texier, A. Foucaud, *Tetrahedron Lett.* **1982**, *23*, 4927.

[65] G. Bartoli, M. Bosco, A. Carlone, R. Dalpozzo, P. Galzerano, P. Melchiorre, L. Sambri, *Tetrahedron Lett.* **2008**, *9*, 2555.

[66] J. Barluenga, L. Riesgo, R. Vicente, L. A. Lopez, M. Tomas, *J. Am. Chem. Soc.* **2007**, *129*, 7772.

[67] J. S. Yadav, B. V. Subbareddy, D. N. chary, C. Madavi, A. C. Kunwar, *Tetrahedron Lett.* **2009**, *50*, 81.

[68] T. I. Reddy, R. S. Varma, *Tetrahedron Lett.* **1997**, *38*, 1721.

[69] S. Shanmuganathan, L. Greiner, D. M. P. Dominguez, *Tetrahedron Lett.* **2010**, *51*, 6670.

[70] L. Yang, J. Zhu, F. Xie, X. Peng, B. Lin, Y. Liu, M. Cheng, *Russ. J. Org. Chem.* **2019**, *55*, 1053.

[71] G. Angajala, V. Aruna, R. Subashini, *J. Mol. Struct.* **2020**, *1220*, 128601.

[72] H. Ying, Z. Guan, Y. H. He, N. Louwagie, M. J. Yao, *J. Chem. Res.* **2010**, *34*, 22.

[73] B. C. Ranu, R. Jana, *Eur. J. Org. Chem.* **2006**, *16*, 3767.
[74] N. Lolak, E. Kuyuldar, H. Burhan, H. Goksu, S. Akocak, F. Sen, *ACS Omega* **2019**, *4*, 6848.
[75] E. M. Schneider, M. Zeltner, N. Kranzlin, R. N. Grass, W. J. Stark, *Chem. Commun.* **2015**, *51*, 10695.
[76] S. Ghosh, J. Das, S. Chattopadhyay, *Tetrahedron Lett.* **2011**, *52*, 2869.
[77] G. Angajala, P. Pavan, R. Subashini, *RSC Adv.* **2014**, *4*, 51459.
[78] Otto-Meth-Cohn, B. Narine, B. Tarnowski, *J. Chem. Soc. Perkin.* **1981**, *1*, 1520.
[79] G. M. Morris, R. Huey, W. Lindstrom, M. F. Sanner, R. K. Belew, D. S. Goodsell, A. J. Olson, *J. Comput. Chem.* **2009**, *16*, 2785.
[80] C. P. Malik, M. B. Singh, *Ludiana* **1980**, *39*, 65.
[81] S. Krishnaveni, B. Theymoli, S. Sadasivam, *Food Chem.* **1984**, *15*, 229.

SUPPORTING INFORMATION

Additional supporting information may be found online in the Supporting Information section at the end of this article.

How to cite this article: Angajala G, Aruna V, Subashini R. Visible light induced nano copper catalyzed one pot synthesis of novel quinoline bejeweled thiobarbiturates as potential hypoglycemic agents. *J Heterocyclic Chem*. 2021; 1–15. https://doi.org/10.1002/jhet.4271